AGU PUBLICATIONS

JGR

Journal of Geophysical Research: Solid Earth

RESEARCH ARTICLE

10.1002/2013JB010933

Key Points:

- Postseismic responses of repeaters are examined for the Tohoku-oki earthquake
- A fast loading due to postseismic slip caused increased moment and slip areas
- The phenomenon suggests aseismic-to-seismic transitions in the surrounding area

Supporting Information:

- Readme
- Figures S1–S18

Correspondence to:
N. Uchida,
uchida@aob.gp.tohoku.ac.jp

Citation:
Uchida, N., K. Shimamura, T. Matsuzawa, and T. Okada (2015), Postseismic response of repeating earthquakes around the 2011 Tohoku-oki earthquake: Moment increases due to the fast loading rate, *J. Geophys. Res. Solid Earth*, *120*, doi:10.1002/2013JB010933.

Received 29 DEC 2013
Accepted 26 NOV 2014
Accepted article online 5 DEC 2014

Postseismic response of repeating earthquakes around the 2011 Tohoku-oki earthquake: Moment increases due to the fast loading rate

Naoki Uchida[1], Kouhei Shimamura[1,2], Toru Matsuzawa[1], and Tomomi Okada[1]

[1]Graduate School of Science, Tohoku University, Sendai, Japan, [2]Now at Japan Oil Engineering Co. Ltd, Tokyo, Japan

Abstract We examined the temporal variation of the size of repeating earthquakes related to the 2011 Tohoku-oki earthquake (*M*9.0) in the northeastern Japan subduction zone for the period from July 1984 to the end of 2011. The repeaters (*M*2.5–6.1) show postseismic magnitude increases for most sequences located in the area of large postseismic slip at the downdip extension of the *M*9 source region. The magnitudes of the first events after the *M*9 earthquake increased by an average of about 0.3 for sequences having three or more earthquakes over the 9 months following it. We also examined the slip area in detail for Kamaishi repeaters whose magnitudes had been *M*4.9 ± 0.2 but which increased by about 1 after the *M*9 earthquake. Waveform modeling shows that the slip area for the post-*M*9 Kamaishi earthquakes overlaps with that before the Tohoku-oki earthquake but enlarged by about 6 times. Until the occurrence time of the last event (September 2011) in the analysis period, the rupture area remained larger than before but appeared to shrink over time. The enlargement of the rupture area suggests that an aseismic-to-seismic transition occurred in the region surrounding the pre-*M*9 repeaters and is most likely related to fast loading of the repeaters due to rapid postseismic slip estimated to have occurred in the area. The existence of conditionally stable regions around the repeating earthquakes and/or patches slightly larger than the earthquake nucleation sizes may explain such behavior. The temporal change of loading rate is an important factor in determining earthquake size in this case.

1. Introduction

The Kamaishi repeating earthquake sequence on the plate boundary offshore Tohoku (Figure 1) exhibited a regular recurrence interval (5.5 ± 0.7 years) and magnitude (*M*4.9 ± 0.2) before the 2011 Tohoku-oki earthquake [e.g., *Matsuzawa et al.*, 2002; *Uchida et al.*, 2005]. These earthquakes are identified based on relocated hypocenters [*Matsuzawa et al.*, 2002], and almost complete overlapping of their slip areas was confirmed from waveform modeling [*Okada et al.*, 2003; *Shimamura et al.*, 2011], although there is some heterogeneity in the slip distributions [*Shimamura et al.*, 2011]. On 20 March 2011, 9 days after the M_w9.0 Tohoku-oki earthquake, an earthquake with a magnitude about 1 unit larger than the average magnitude before the Tohoku-oki earthquake (*M*5.9) occurred in the earthquake cluster. The *M*5.9 event was followed by five *M*5.0–5.5 events (post-Tohoku events) over about 6 months at intervals that tended to lengthen over time (Figure 2). If these post-Tohoku events belongs to the same repeater sequence as the earthquakes before the Tohoku-oki earthquake (pre-Tohoku events), the short recurrence interval is natural because postseismic slip of the Tohoku-oki earthquake may have triggered the earthquakes. However, the larger size of the earthquakes is not explained simply with a general repeating earthquake model (recurrent ruptures of the same seismic patch surrounded by an aseismic slip area). The size increase requires an enlargement of the slip area or slip amount or both.

In addition to the Kamaishi sequence, there are many small repeating earthquakes in the northeastern Japan subduction zone [e.g., *Igarashi et al.*, 2003]. These small repeating earthquakes were identified by conducting a systematic search for events with very high waveform similarity. These small repeating earthquakes, similar to the Kamaishi repeating earthquakes, suggest overlapping rupture areas and are thought to be recurrent ruptures of seismic patches surrounded by an aseismic slip area. There have been many efforts to study the cycle of large earthquakes using paleoseismic data [*Weldon et al.*, 2004], historical data [*Ishibashi*, 1999], geodetic data [*Murray and Langbein*, 2006], and seismic data [*Yamanaka and Kikuchi*, 2004]. However, how the earthquake size varies for earthquakes in the same patch/section is not well known [e.g., *Rubinstein et al.*, 2012]. The use of small repeating earthquakes for this purpose has the

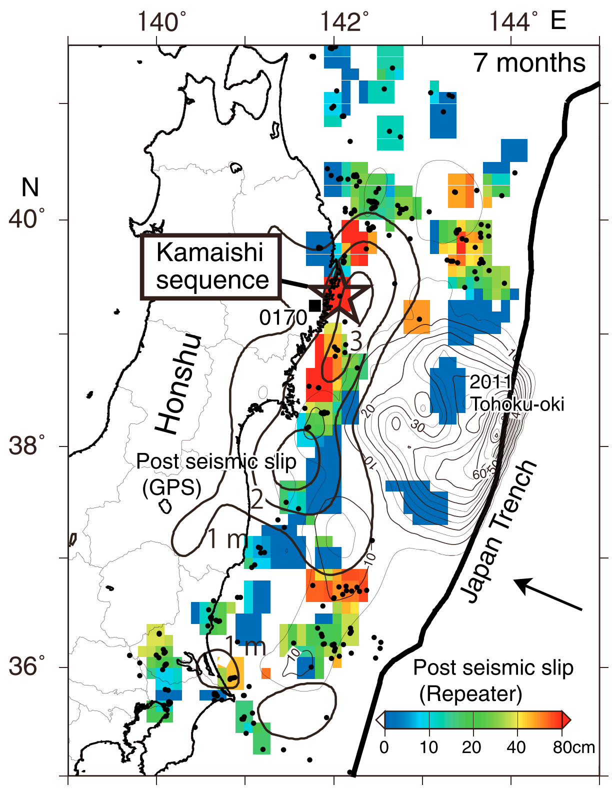

Figure 1. Location of the Kamaishi earthquake sequence (open star), small repeating earthquake sequences studied in this paper (black dots), and postseismic slip of the 2011 Tohoku-oki earthquake over 7 months. The postseismic slip estimated from GPS data [*Ozawa et al.*, 2012] and repeating earthquake data [*Uchida and Matsuzawa*, 2013] are shown by thick contours and color, respectively. The coseimic slip distribution for the Tohoku-oki earthquake from land and offshore GPS data is also shown by thin contours [*Iinuma et al.*, 2012]. The black square denotes the GPS station (0170) whose movement is plotted in Figure S3.

advantage that they occur more frequently than larger ones. Both small repeating earthquakes and large megathrust earthquakes occur with the same faulting mechanism and on the same plate boundary. Therefore, studying how the magnitude of small repeaters varies has great implications not only on the variation of earthquake sizes that occurs on the same patch/section of the fault plane but also on the mechanism of earthquake size variation in general. After the Parkfield earthquake, there were repeater sequences in which moment increased and others where moment decreased [*Chen et al.*, 2010]. These phenomena were explained through a simulation using a rate and state friction law. Repeating earthquake data, especially in the period after a large earthquake, teach us about the frictional properties of the fault zone.

In this study, we examine changes in repeating earthquake size in the period from 1984 to the end of 2011 when rapid postseismic slip was observed. We quantify the earthquake magnitude changes before and after the 2011 Tohoku-oki earthquake for many small repeating earthquakes offshore Tohoku then model the source process for the Kamaishi earthquake sequence in order to estimate the role of the postseismic slip of the Tohoku-oki earthquake.

2. Spatial Distribution of Magnitude Change for Small Repeating Earthquakes

To study the size change of small repeating earthquakes systematically, we first examined the change in magnitude of a large data set of small repeating earthquakes before and after the Tohoku-oki earthquake. We used repeating earthquakes catalogued by *Uchida and Matsuzawa* [2013] for the period from July 1984 to December 2011. The magnitudes in the catalogue are taken from the Japan Meteorological Agency's earthquake catalogue. The criteria for designating repeaters are the following: (1) their average coherence in the 1 to 8 Hz passband must be larger than 0.95 for *M*2.5 to *M*4.0 events and (2) the average coherence at half to double the corner frequency must be larger than 0.8 for earthquakes larger than *M*4.0. Here we used waveforms during a 40 s time window. There are no criteria for the interval or duration of the repeating earthquake sequences. The catalogue has 316 sequences that were active both before and after the Tohoku-oki earthquake (black dots in Figure 1). This data set captures repeater activity during a 27 year period before and a 9 month period after the Tohoku-oki earthquake.

The average magnitude of repeating earthquakes after the Tohoku-oki earthquake increased for many sequences around the rupture area (Figure 3). The increases were prominent for sequences that had multiple repeating earthquakes after the Tohoku-oki earthquake (large circles in Figure 3). These repeaters are mostly located in deep parts of the distribution of interplate seismicity. The magnitudes of some repeaters along the trench (occurring on the shallow plate boundary) decreased, although the number of earthquakes after the Tohoku-oki earthquake is relatively small for these repeating earthquakes. Note that average magnitude change is not accurate for sequences with small numbers of events. Note also that if repeaters' magnitude

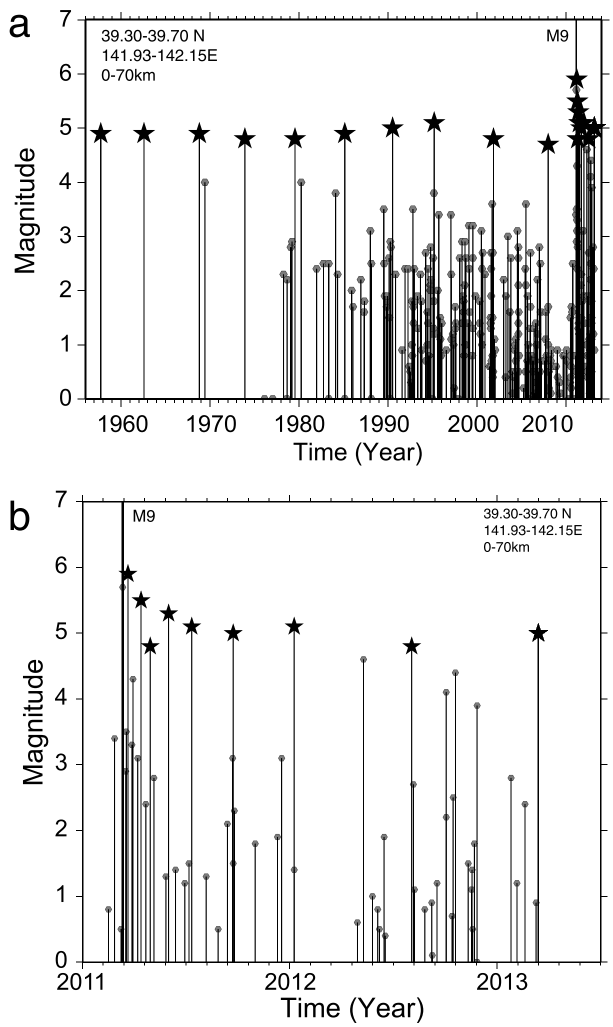

Figure 2. Magnitude-time plot for the off-Kamaishi region. (a) Entire period (1956 to 9 March 2013) and (b) enlargement for the period from 2011 to 9 March 2013. The vertical line shows the time the 2011 Tohoku-oki earthquake occurred. Earthquakes belonging to the Kamaishi sequence are denoted by stars. The *M*5.7 event on 11 March is a little far away from the sequence and was excluded from the sequence. Note that the lack of small earthquakes, especially from 1956 to 1995, is due to poor detectability of smaller earthquakes.

changes are too large, their waveforms may become dissimilar and not be registered as members of a repeating sequence. Such waveform perturbation occurred in the Kamaishi sequence so that some of the earthquakes in the sequence after the Tohoku-oki earthquake were not recognized as repeaters based on velocity waveform similarity. We will discuss this sequence in sections 3 and 4.

The increased frequency of occurrence of repeating earthquakes from the same sequence after the Tohoku-oki earthquake (shown by circle size in Figure 3) indicates the existence of rapid postseismic slip that loaded small asperities, causing them to rupture at shorter recurrence intervals. This suggests that fast postseismic slip is probably also related to the magnitude increases the repeaters undergo. The correlations between the increased-magnitude sequences and postseismic slip from GPS data (Figures 1 and 3) also confirm the relationship. There are many sequences with magnitude increases (red circles in Figure 3) in the area where the GPS data suggest postseismic slip of 1 m in 7 months after the Tohoku-oki earthquake as indicated by the pink contour in Figure 3. As examples, Figure 4 shows magnitude-time relationships for eight sequences that have large numbers of earthquakes after the Tohoku-oki earthquake (Figure 3). Seven of these have increased magnitudes, and the other has decreased magnitudes (Figure 4). The magnitude-decreased sequence has a relatively small number of earthquakes before the Tohoku-oki earthquake and is thus less reliable than the other sequences. This also applies to sequences f and h.

There were no prominent earthquake-magnitude changes other than in the period around 1995 for regions a–c. This corresponds to the period after the *M*7.6 Sanriku-oki earthquake on 28 December 1994 (vertical lines in Figures 4a–4c), which is the second largest earthquake along the Japan trench in the study period. This earthquake also showed significant postseismic slip near the slip area (contours in Figure 3), including the locations of sequences a–c [*Heki et al*., 1997; *Nishimura et al*., 2000; *Uchida et al*., 2004].

Comparing the repeating earthquake magnitudes of the first, second, and third events after the Tohoku-oki earthquake with previous earthquakes suggests that there was a change at the time of the Tohoku-oki earthquake (Figure 5). The average and median magnitudes for the first event after the Tohoku-oki earthquake (sequence number 1) are about 0.3 larger than before (sequence numbers −3, −2, and −1) for repeating earthquake sequences that have three or more earthquakes both before and after the Tohoku-oki earthquake (Figure 5). This magnitude increase (0.3) corresponds to about a 2.8 times larger seismic moment. To check this average magnitude change, we performed Welch's *t* test for the data set before and after the Tohoku-oki earthquake. The result indicates that the mean difference is statistically significant at a 99% confidence level.

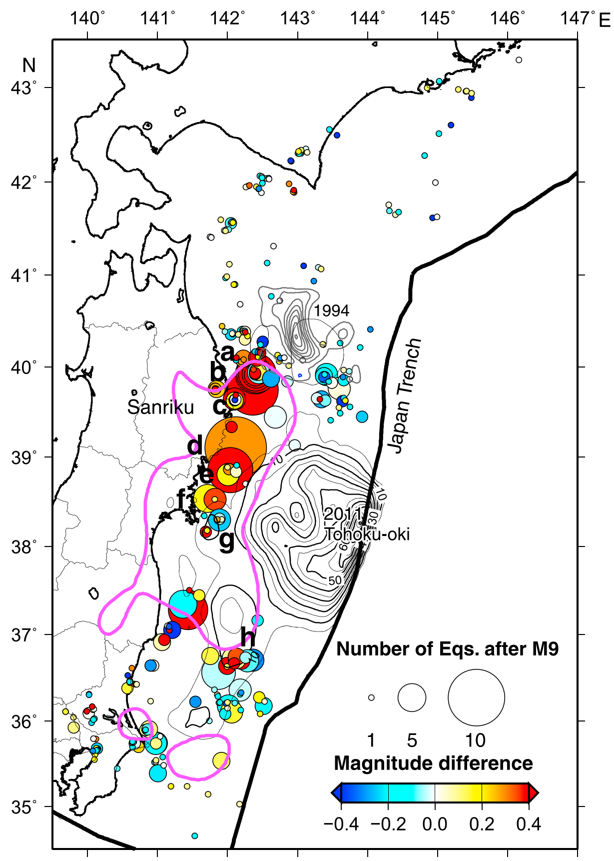

Figure 3. Average magnitude difference (post-Tohoku minus pre-Tohoku) for each repeating earthquake sequence. Circle size shows the number of earthquakes after the Tohoku-oki earthquake. Earthquakes from July 1984 to 31 December 2011 were used for the analysis. Black contours show the coseismic slip distributions of the 2011 Tohoku-oki earthquake [*Iinuma et al.*, 2012] and the 1994 Sanriku-oki earthquake [*Nagai et al.*, 2001]. The pink contour line indicates 1 m postseismic slip over 7 months after the Tohoku-oki earthquake estimated from GPS data [*Ozawa et al.*, 2012].

We also show the distribution of the relative magnitude before and after the Tohoku-oki earthquake in Figure S1 in the supporting information. The increase of complete magnitude (i.e., change in detectability) may also cause an apparent magnitude change. However, the magnitude change is still significant even if we use a data set with relatively large repeaters (mean magnitude ≥ 3.0; see also Figure S2). Thus, the result suggests that the magnitude change is real. The standard errors of the relative magnitudes (error bars in Figure 5) show a little more scatter for post-Tohoku repeaters, which is validated by an *F* test at a 99% significance level (see also Figure S1). The average and median magnitudes slightly decrease after the first post-Tohoku event. A temporal distribution of relative magnitude on a linear time scale clearly shows the positive change in relative magnitude at the time of the Tohoku-oki earthquake (Figure S3). The temporal change correlates well with the ground velocity changes (Figure S3).

3. Comparison of the Source Process of the Kamaishi Earthquakes

The earthquakes in the Kamaishi earthquake cluster were larger and more frequent after the 2011 Tohoku-oki earthquake (Figure 2). The magnitude-time plot for a small area off Kamaishi, shown in Figure 2, includes data before and after the small repeater analysis period (from July 1984 to the end of 2011). The magnitudes of events came back to the level of the period before the Tohoku-oki earthquake by the end of 2011. Before the Tohoku-oki earthquake, the waveforms of the Kamaishi sequence were very similar (Figure 6, 2001 and 2008 events). We plotted only two pre-Tohoku waveforms in Figure 6 because the KiK-net stations used in this study were installed in 2001, but waveform and magnitude similarity have been confirmed in previous studies using other network data [e.g., *Matsuzawa et al.*, 2002; *Okada et al.*, 2003]. The waveforms after the Tohoku-oki earthquake, however, differed from the previous ones (Figure 6). Here we consider earthquakes with magnitude 4.7 or larger since 2008, and if they overlap with the 2008 event, we consider them to be repeating earthquakes. Whether the source areas of the Kamaishi earthquakes overlap even after the Tohoku-oki earthquake (i.e., they belong to the same repeating earthquake sequence that *Matsuzawa et al.* [2002] found off Kamaishi) has not yet been checked [*Ye et al.*, 2012]. If they belong to the repeating earthquake sequence, we may study the effect of slip rate change in the surrounding area [*Ozawa et al.*, 2011; *Uchida and Matsuzawa*, 2013] on the rupture process. In this section, we will estimate the spatial distribution of the source areas of the events after 2008 shown in Figure 6 and investigate the relationship between the distribution and postseismic slip of the Tohoku-oki earthquake.

3.1. Relocation of the Kamaishi Earthquakes

To examine the earthquake activity after the Tohoku-oki earthquake in more detail, we performed hypocenter relocations. To determine hypocenters precisely, we first determined *P* and *S* wave onsets

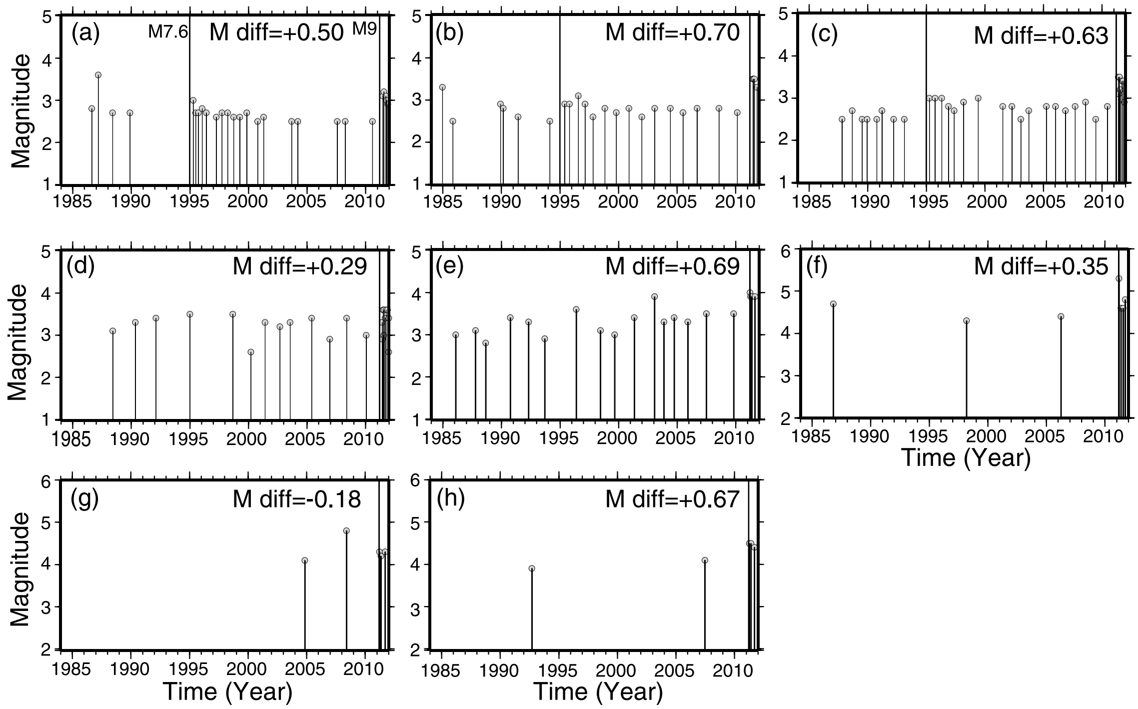

Figure 4. (a–h) Magnitude-time plots for several repeating earthquake sequences labeled in Figure 2. The vertical lines show the timing of the 2011 Tohoku-oki earthquake and the 1994 Sanriku-oki earthquake (*M*7.6).

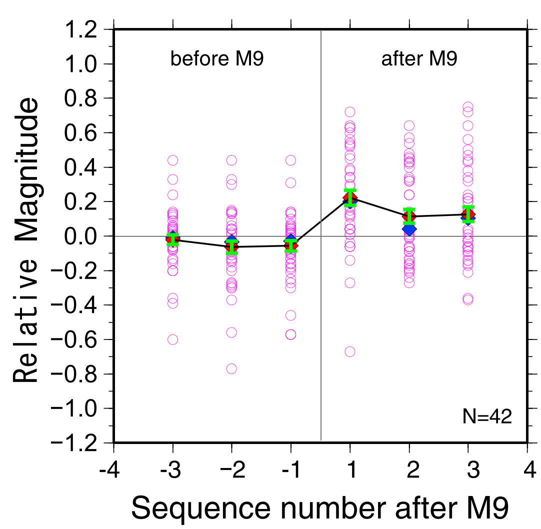

Figure 5. Evolution of the magnitudes of repeaters before and after the 2011 Tohoku-oki earthquake. The difference in magnitude (relative magnitude) between each event and the average of its sequence was plotted versus its sequential number after the Tohoku-oki earthquake. Negative sequence numbers denote earthquakes before the Tohoku-oki earthquake. Pink circles mark the magnitudes of individual earthquakes. Red diamonds and green error bars show averages and standard errors, respectively. Blue diamonds show median values. The 42 sequences with three or more earthquakes both before and after the Tohoku-oki earthquake (until December 2011) were plotted.

manually using the method proposed by *Shimamura et al*. [2011]. The precise hypocenter locations are quite important for comparing the slip distributions of different earthquakes that will be described in section 4. Note that the waveform correlation method [e.g., *Waldhauser and Ellsworth*, 2000] is not suitable for this analysis because it is useful to estimate the relative locations of the centroids of the slip distributions, but here we need the precise locations of rupture initiation points. The Shimamura's method is summarized as follows. We can read *S* wave onsets precisely by taking into consideration that the double difference (DD) of *S* wave arrival times should be the product of the DD of *P* wave arrival times and a V_P/V_S ratio (*P* and *S* wave velocity ratio):

$$\left(t^1_{S,a} - t^1_{S,b}\right) - \left(t^2_{S,a} - t^2_{S,b}\right) = \gamma\left\{\left(t^1_{P,a} - t^1_{P,b}\right) - \left(t^2_{P,a} - t^2_{P,b}\right)\right\} \quad (1)$$

where t_P and t_S are, respectively, the arrival times of *P* and *S* waves and γ is the V_P/V_S ratio. Superscripts 1 and 2 indicate earthquakes, and subscripts *a* and *b* indicate stations. This equation shows that the arrival time double difference must be located on a straight line with a slope corresponding to the V_P/V_S ratio. Although this is

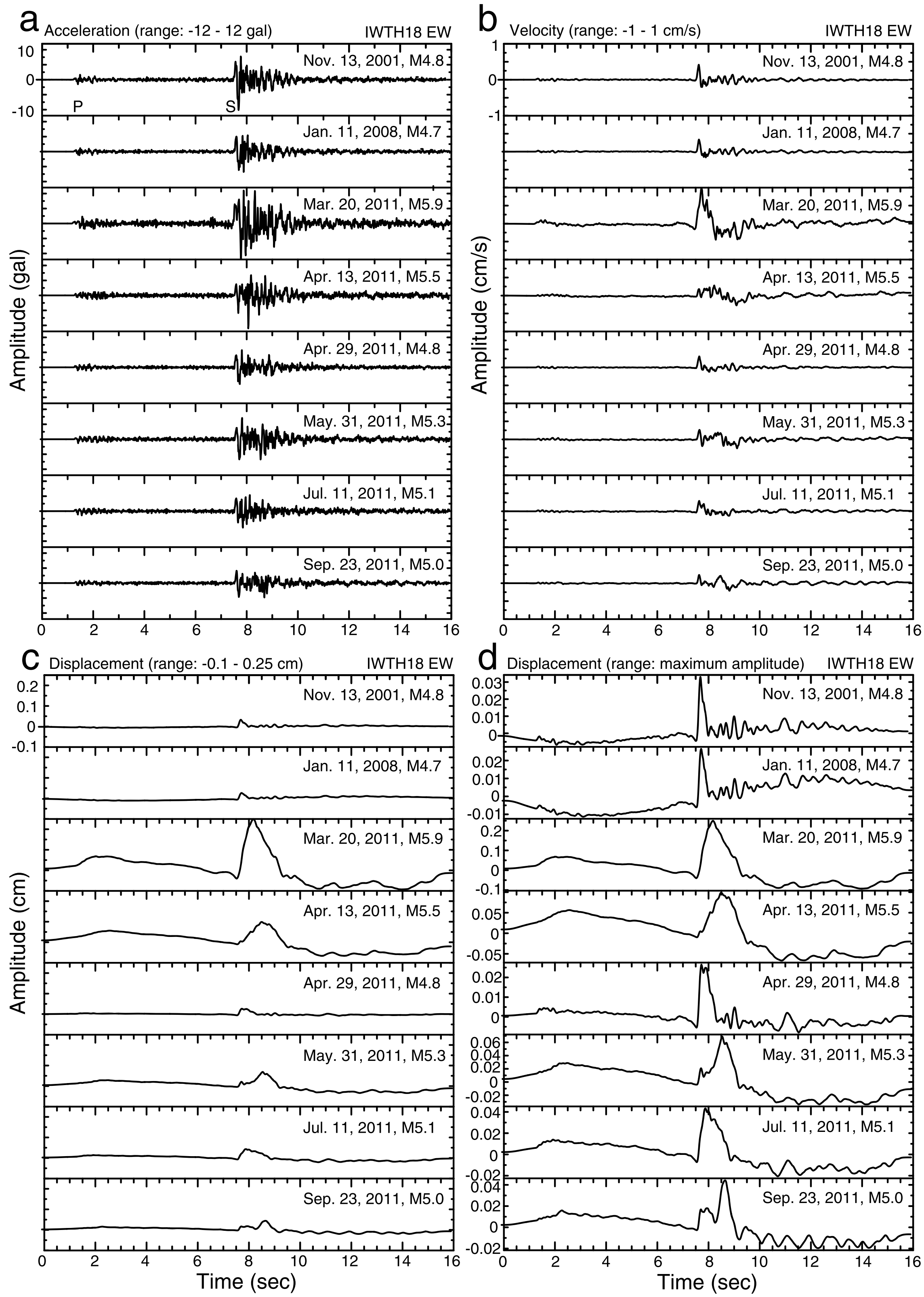

Figure 6. Waveform examples of the earthquakes belonging to the Kamaishi sequence from 2001 to 23 September 2011 recorded at KiK-net station IWTH18 (Figure 7a). The component is east-west, and sampling frequency is 100 Hz. (a) Acceleration seismogram. (b) Velocity seismogram. (c and d) Displacement seismograms. In Figures 6a–6c, seismograms are plotted in the same amplitude scale for each figure, while the seismograms in Figure 6d are normalized by the maximum amplitudes for the respective traces. *P* and *S* wave arrivals are marked in Figure 6a. No filtering was applied.

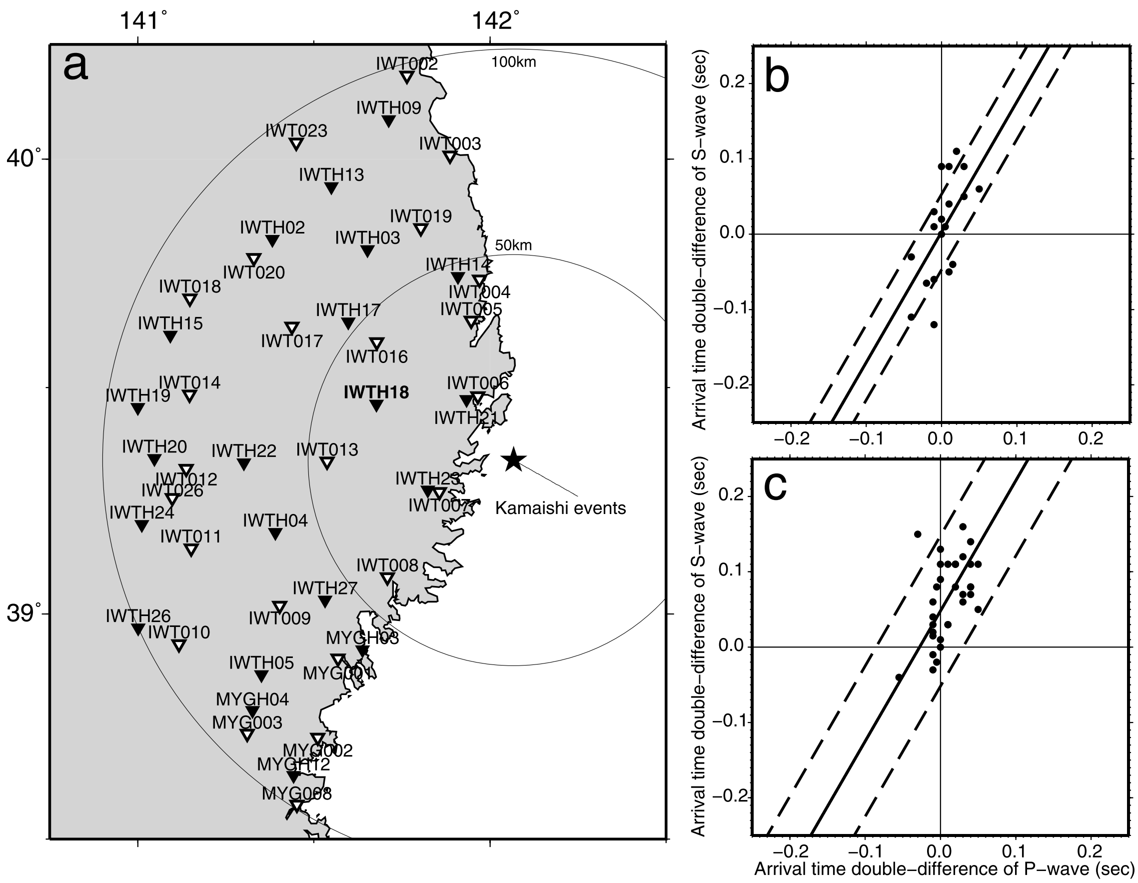

Figure 7. (a) Distribution of stations used for relocation and source process estimation. Open and solid triangles, respectively, denote K-NET and KiK-net stations. The black star shows the location of the Kamaishi earthquake sequence. Examples of the arrival time double differences between (b) the 2008 *M*4.7 event and the 27 February 2011 *M*3.4 event and (c) the 20 March 2011 *M*5.9 event and the 2008 *M*4.7 event. Horizontal and vertical axes show *P* and *S* wave arrival time double differences, respectively. Station IWTH18 (Figure 7a) was selected as a reference, and all available stations paired with IWTH18 are plotted here. The solid line shows the best fit regression line with a slope of 1.73. The dashed lines in Figures 7b and 7c, respectively, show 0.0 and 0.1 s error limits used for the rupture process analysis.

true only if the V_P and V_S structures are the same along the raypaths to each station, we utilized this idea to check for phase reading outliers. We plotted the double differences, i.e., $\left(t^1_{S,a} - t^1_{S,b}\right) - \left(t^2_{S,a} - t^2_{S,b}\right)$ versus $\left(t^1_{P,a} - t^1_{P,b}\right) - \left(t^2_{P,a} - t^2_{P,b}\right)$, for all available station pairs on one figure for each earthquake pair. We selected outliers (points far from the best fit line) and reread or discarded the phase readings depending on the quality of the waveform.

We used seismic data from Kiban Kyoshin network (KiK-net) and Kyoshin network (K-net) stations operated by the National Research Institute for Earth Science and Disaster Prevention (NIED) for reading phases (Figure 7a). Figures 7b and 7c show examples of arrival time double differences of *P* and *S* wave first motions manually picked by the authors. The *S* wave data have more scatter than do the *P* wave data. Based on seismic tomography results in this region [*Tsuji et al.*, 2008], the V_P/V_S value (slope) was fixed to 1.73 and fitted to the data (Figures 7b and 7c). The arrival time improvement is also important for empirical Green's function analysis to estimate the rupture process that is described in the next section. To estimate the slip evolution of an earthquake, we need good *S* wave onset data. Therefore, we set a threshold for acceptable data to be about 1/10 of the rise time for rupture process analysis, which is similar to the time interval of the basis function used in the analysis (see next section for details). As a result, we selected *S* wave data within 0.05 s for the two smallest events (the 2008 *M*4.7 and the 29 April 2011 *M*4.8 earthquakes) and 0.1 s for other events from the respective best fit lines. The differences between the thresholds are due to the difference in the source time durations: ~0.5 s for the *M*4.7

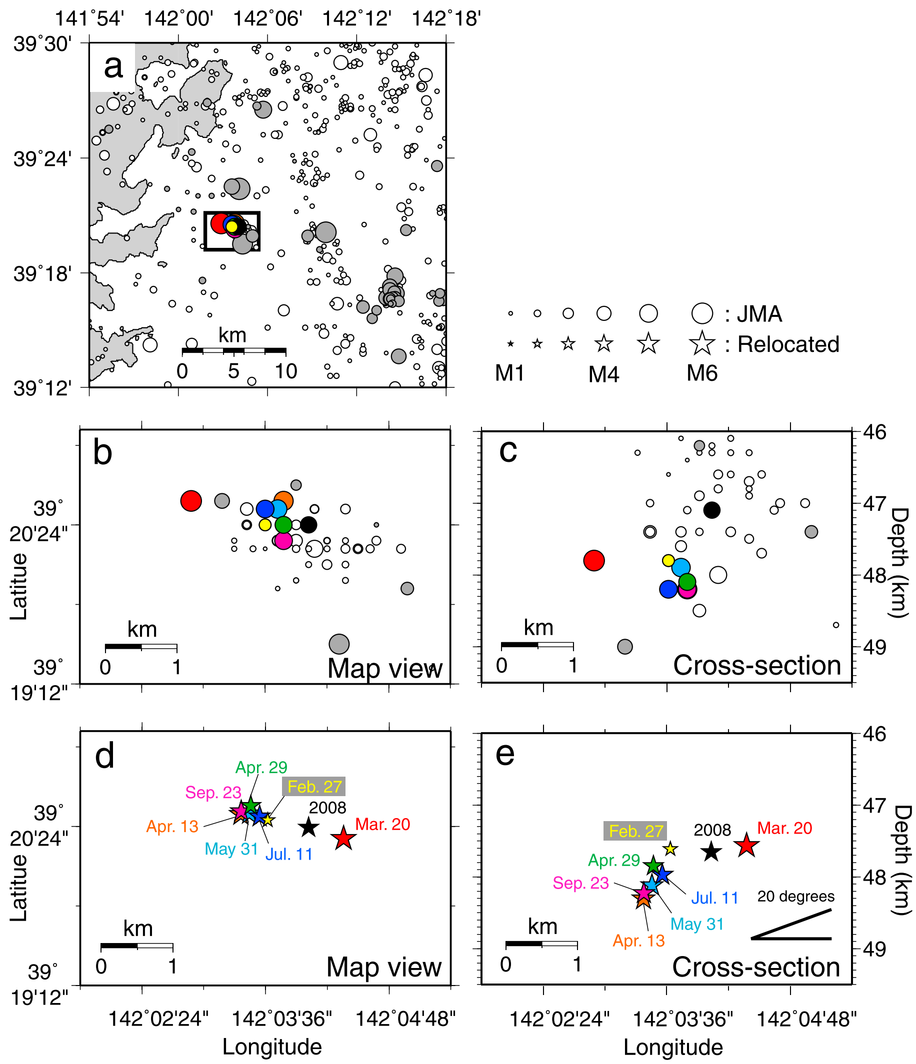

Figure 8. Hypocenter distribution for the off-Kamaishi area according to the JMA catalogue and relocated hypocenters. Colored circles denote the Kamaishi sequence earthquakes, and gray circles are earthquakes that occurred after the Tohoku-oki earthquake. (a) Epicenter distribution for the period from 1 January 2001 to 23 September 2011 for earthquakes of *M*1 or larger. Land area is shown in gray. (b) Close up of the original JMA epicenter distribution in the rectangle in Figure 8a. (c) East-west vertical cross section of the original JMA hypocenter distribution in the rectangle. (d) Relocated epicenters for the Kamaishi sequence. (e) Vertical cross section of the relocated hypocenter distribution.

and*M*4.8 events and 1–2 s for larger events as shown in Figure 6. If the time difference between an *S* wave onset and the best fit line exceeded the threshold, we tried to repick the onset. If no other candidates were found, we dismissed the datum.

Using the refined phase data, we relocated earthquakes in the earthquake cluster by employing a double-difference method [*Waldhauser and Ellsworth*, 2000] (Figure 8). The relocated hypocenters are within 2 km and are aligned in the east-west direction. The depth distribution shows the earthquakes on an ~20° west dipping plane that is probably the surface of the subducting Pacific plate (Figure 8e). The focal mechanisms of these earthquakes, determined by the Full Range Seismograph Network of Japan (F-net) are low-angle thrust type, consistent with the hypocenter alignment. All the earthquakes are within 1 km from the 2008 event (black star).

3.2. Estimation of the Source Process of the Kamaishi Earthquakes

The displacement waveforms of the Kamaishi sequence (Figures 6c and 6d) show broader *S* wave pulses and larger amplitudes after the Tohoku-oki earthquake. This suggests different rupture processes from those

Table 1. Kamaishi Sequence Event List and Analysis Parameters

Date			M	Strike[a] (deg)	Dip[a] (deg)	Rake[a] (deg)	Date of EGF			EGF M	Frequency Range (Hz)	Grid Spacing (km)	Interval of Basis Functions (s)	Maximum Rupture Speed (km/s)
2008	1	11	4.7	189	19	77	2011	2	27	3.4	1–5	0.5	0.05	3.8
2011	3	20	5.9	182	21	67	2008	1	11	4.7	0.5–2	1.0	0.15	3.0
2011	4	13	5.5	173	21	59	2008	1	11	4.7	0.5–2	1.0	0.15	3.0
2011	4	29	4.8	190	20	80	2011	2	27	3.4	1–5	0.5	0.05	3.8
2011	5	31	5.3	178	24	63	2008	1	11	4.7	0.5–2	1.0	0.15	3.0
2011	7	11	5.1	189	20	74	2008	1	11	4.7	0.5–2	1.0	0.15	3.0
2011	9	23	5.0	177	21	62	2008	1	11	4.7	0.5–2	1.0	0.15	3.0

[a]The fault parameters (strike, dip, and rake) are from the F-net catalogue.

before. To estimate the slip distributions of the Kamaishi earthquakes on the plate boundary, we used the multiple time window waveform inversion method [*Hartzell and Heaton*, 1983; *Shimamura et al*., 2011] and applied it to the KiK-net and K-net acceleration seismograms [*Shimamura*, 2012] (Figure 7a). In this method, many grid points are set on an assumed fault plane and observed waveforms are inverted to determine the moment release histories at respective grid points. The rupture front is assumed to propagate in a circular manner at the "maximum" rupture velocity, and the moment rate function for each grid point is assumed to be expressed as a linear combination of basis functions that are isosceles triangles with base τ. The interval between the isosceles triangles is set to be half of τ. Thus, the unknown parameters are the heights of these isosceles triangles. Three-component waveforms with 5 s windows for both *P* and *S* waves are used for the analysis (Figures S11–S17).

In order to stabilize the inversions, we applied a priori constraints on the smoothness of temporal and spatial changes and on the absolute values of unknown parameters. For the smoothness of temporal changes, the second-order time derivatives of unknown parameters were assumed to be almost zero at each grid point. For the smoothness of spatial changes, the two-dimensional Laplacians of unknown parameters were assumed to be very small. A weak damping of the absolute values was also adopted to stabilize the inversion. We used two empirical Green's functions (EGF) [e.g., *Hartzell*, 1978] as listed in Table 1, the *M*3.4 event on 27 February 2011 for $M < 5$ events and the 4.7 event on 11 January 2008 for $M \geq 5$ events. The uses of smaller EGF (*M*3.4) for the larger events were not appropriate because of the low signal-to-noise ratio of the EGF in the low-frequency range. Other parameters (frequency range, grid spacing, interval of basis functions, and maximum rupture speed) are also listed in Table 1. The procedures used in their determination are explained in the supporting information. The strike and dip angles for the fault planes listed in the table are taken from the F-net focal mechanism catalogue.

Figure 9 shows the inversion results for seven Kamaishi earthquakes from 2008 to 2011. The results of temporal evolutions of slip are shown in the supporting information (Figures S4–S10). The modeled to observed fits are generally good (Figures S11–S17). The 2008 event (*M*4.7) has a rupture area with a diameter of about 1.2 km, and the maximum slip occurred west of the hypocenter (Figure 9a). The 20 March 2011 event (the first one after the Tohoku-oki earthquake) showed a slip area of about 8 km in diameter, with the maximum slip located east of the hypocenter (Figure 9b). The 13 April 2011 (*M*5.5, Figure 9c), 31 May 2011 (*M*5.3, Figure 9e), 11 July 2011 (*M*5.1, Figure 9f), and 23 September 2011 (*M*5.0, Figure 9g) events also have larger slip areas than the 2008 event. The 29 April 2011 event (*M*4.8, Figure 9d) had a slip area of 1.6 km in diameter with maximum slip located west of the hypocenter (Figure 9d). This is similar to the size of the pre-Tohoku events ($M \sim 4.9$). We superimposed the slip distributions for the seven earthquakes on a map using their hypocenters as relocated in this study (Figure 10a). The events after the 2011 Tohoku-oki earthquake ruptured not only in the source area of the 2008 event (black in Figure 10a) but also a much larger area, except for the 29 April 2011 event (light green in Figure 10a). The slip expansion is prominent to the east of the 2008 source area (Figure 10a). The cumulative slip for all the earthquakes is shown in Figure 10b. The maximum cumulative slip of about 1.4 m is located to the west of the hypocenter of the 2008 Kamaishi earthquake (black star), and the area showing slip larger than 1.2 m corresponds to the source area of the 2008 earthquake.

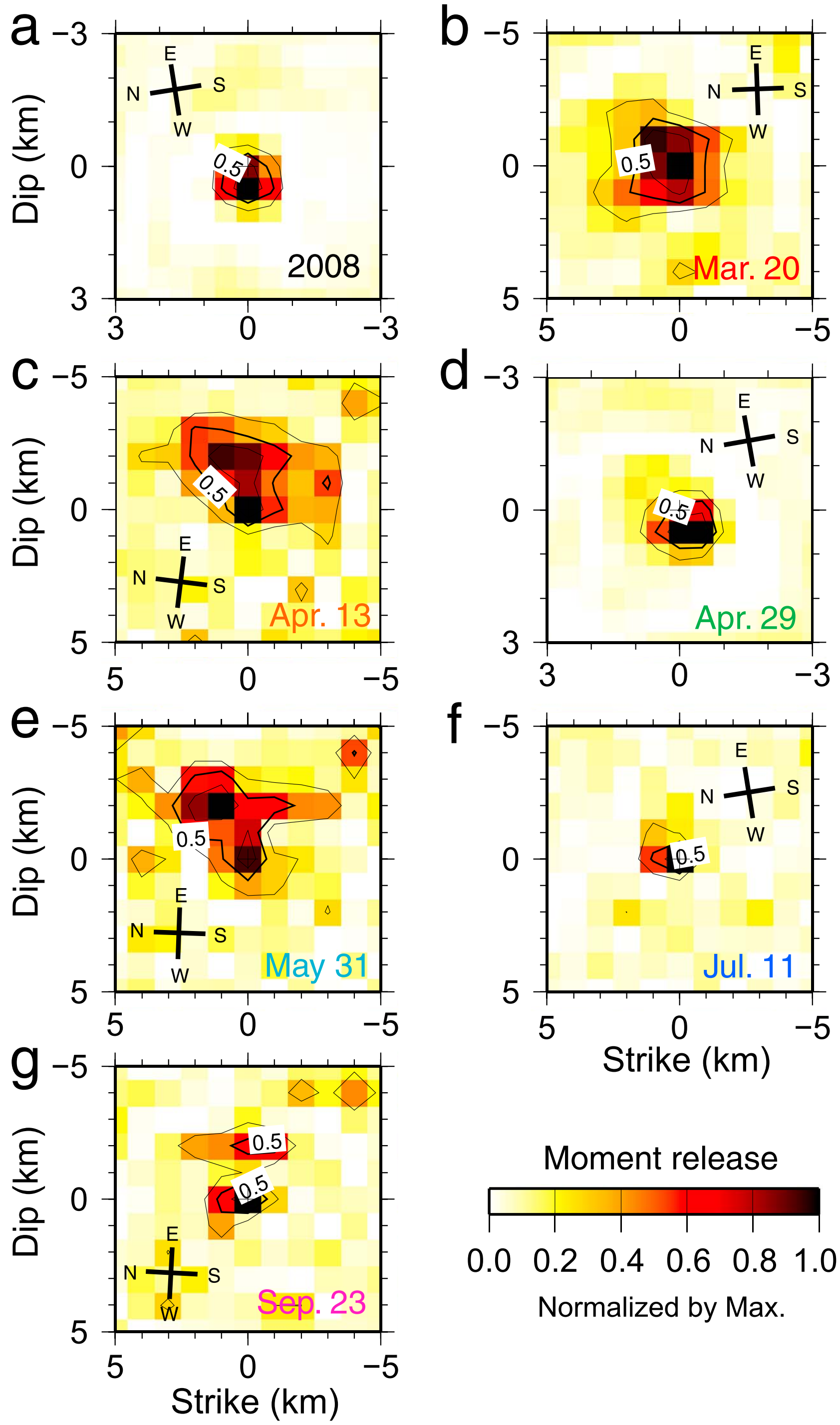

Figure 9. (a–g) Spatial distribution of the total moment release for seven Kamaishi earthquakes from 2008 to 2011. The origin of the axes is the hypocenter of the earthquake. Due to an inclined fault plane, the compass directions (N, S, E, and W) shown in the panels are true for the strike direction but approximate for the dip direction.

In addition to this, a relatively large slip of about 1 m is located east of the 2008 hypocenter. In this inversion, the maximum rupture speed is not constrained well as shown in Figure S18. Even if we use a different speed with a realistic range of 2.3–4.8 km/s, however, the relative locations and ratio of source areas of the events discussed above will not change.

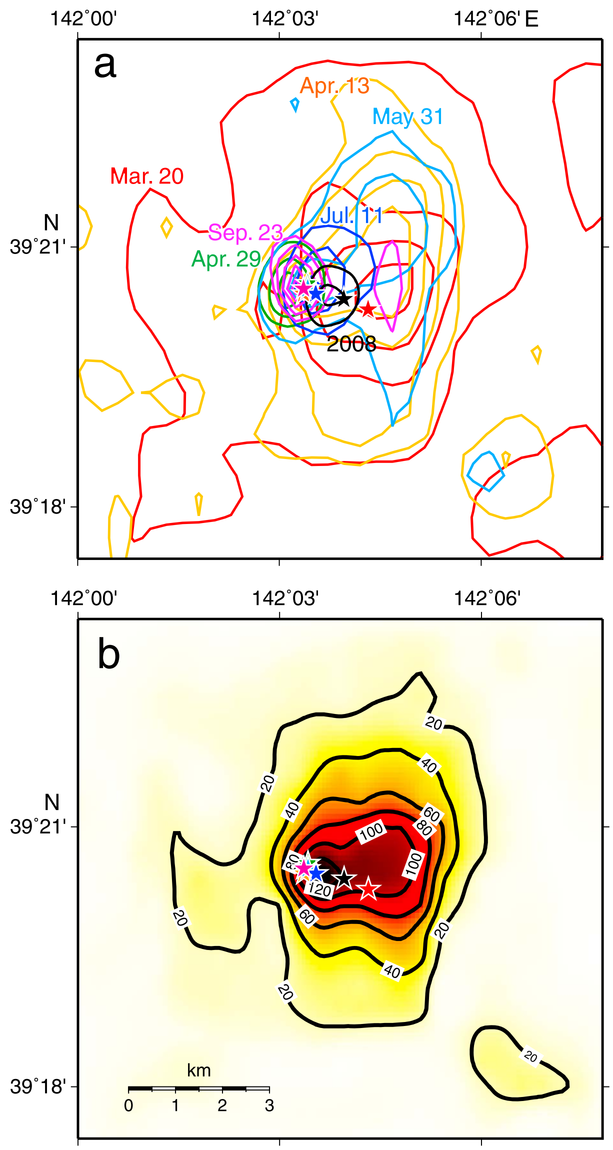

Figure 10. (a) Slip distributions for the seven Kamaishi earthquakes in the map view. Black: 11 January 2008 earthquake, Red: 20 March 2011, Orange: 13 April 2011, Green: 29 April 2011, Light blue: 31 May 2011, Blue: 11 July 2011, Pink: 23 September 2011. The contours start at 5 cm and intervals are 20 cm for the 20 March 2011 event (red) and 5 cm for the other events. The stars with the same color as the contours are epicenters relocated in this study. A shear modulus of 50 GPa was used to calculate the slip from the seismic moments. (b) Cumulative (total) slip for all seven earthquakes shown in Figure 10a. Stars denote the epicenters as in Figure 10a.

4. Discussion

In this study, we observed that repeaters' magnitudes increased after the Tohoku-oki earthquake for many repeating earthquake sequences. The magnitude increase is prominent near the Sanriku coast (Figure 3). In this area, previous studies show the activity of large earthquakes to be low [*Matsuzawa et al.*, 2002; *Ye et al.*, 2012], and relatively small locking has been estimated from GPS data [*Hashimoto et al.*, 2009; *Loveless and Meade*, 2010; *Nishimura et al.*, 2000; *Suwa et al.*, 2006] and from repeating earthquakes [*Uchida and Matsuzawa*, 2011]. The large postseismic slip of the Tohoku-oki earthquake in this area can be explained by the halt of the coseismic slip in the mostly creeping area because of its slip rate hardening nature [*Uchida and Matsuzawa*, 2011; *Ye et al.*, 2012] and stress increases in the area due to the coseismic slip. The postseismic slip amounted to 2 m in 6 months [*Ozawa et al.*, 2012] near the Kamaishi sequence, which is comparable to the maximum cumulative slip of the Kamaishi earthquakes estimated in this study (1.4 m in 6 month and 12 days, Figure 10b).

We hypothesize that the small repeating earthquakes, including the Kamaishi earthquake sequence, occur at small asperities on the plate boundary loaded by aseismic slip in the surrounding region. In that case, repeaters' recurrence intervals shorter than usual suggest an increased loading rate at the asperity where the repeaters occur if the asperity strength does not change. Since the mean interval of the Kamaishi repeating earthquakes before 2011 was 5.5 years, the occurrence of multiple earthquakes within 9 months after the Tohoku-oki earthquake suggests an increased loading rate there. The synchronicity of the increased magnitudes and decreased repeating intervals strongly suggests that the loading rate increase also caused the postseismic repeater magnitude increase. The spatial correlation between postseismic slip estimated from GPS data and distribution of magnitude-increased sequences also support this idea. Other possibilities include (1) pore pressure decreases that increases the instability in velocity-weakening regions and (2) mode changes from separate to simultaneous ruptures of multiple locked areas. For the first hypothesis, the water could have escaped from the plate boundary fault because of the strong shaking due to the Tohoku-oki earthquake and dilatational coseismic stress change in the overriding plate. In this case, however, the pore pressure should have remained lower than usual after the Tohoku-oki earthquake, and thus, the source size should also have remained larger than usual. This does not fit the

Table 2. Estimated Maximum Slip, Radius, and Stress Drop for the Kamaishi Sequence[a]

Date			M	Maximum Slip (cm)	Radius (km)	Stress Drop (MPa)
2008	1	11	4.7	12	0.63–0.65	8.5–8.7
2011	3	20	5.9	71	4.3–4.9	6.6–7.6
2011	4	13	5.5	28	2.6–4.2	3.1–4.9
2011	4	29	4.8	18	0.79–0.89	9.3–10.4
2011	5	31	5.3	15	2.4–2.9	2.4–2.9
2011	7	11	5.1	19	1.0–1.1	7.9–8.7
2011	9	23	5.0	11	1.5–1.8	2.8–3.4

[a]Radius and stress drop ranges are from the 5 cm slip area.

observation that the magnitudes of the Kamaishi earthquakes returned to the previous values within 1 year after the Tohoku-oki earthquake as shown in Figure 2. If the second hypothesis is correct, there should have been a lot of earthquakes around the Kamaishi earthquakes and summed moment for these earthquakes for the one cycle of the Kamaishi sequence should have been comparable to an $M \sim 6$ earthquake. In the study area, however, only small earthquakes except for the Kamaishi sequence had occurred until the Tohoku-oki earthquake (Figure 2); the summed moment for these small events in the one cycle of the sequence was considerably smaller than the enlarged earthquakes ($M \sim 6$) after the Tohoku-oki earthquake.

There are also repeating earthquakes with decreased magnitude, especially near the trench. The differences in fault depth and/or fault property may relate to the difference in the magnitude change. Although most of the repeating earthquakes near the downdip limit (western edge) of repeating earthquake distribution show magnitude increase, several repeaters with decreased magnitude also exist within the 1 m postseismic slip contour especially to the south of the Tohoku-oki coseismic slip (Figure 3). This may reflect local pore pressure changes and/or heterogeneous distribution of frictional parameters. Most of the sequences indicating magnitude decrease, however, show only a small number of repeats after the Tohoku-oki earthquake and thus are less reliable than the other repeaters.

As for the Kamaishi sequence, the increased magnitudes (seismic moments) were caused by both increased slip areas and amounts (Figure 10a and Table 2). As described before, we classify repeating earthquakes in this study as those where slip distribution analysis shows events whose slip area overlaps with those of other earthquakes. All the earthquakes shown in Table 1 and Figure 10a are repeating earthquakes. However, this situation is different from the constant area for repeaters that is sometimes assumed in repeater analysis [*Nadeau and Johnson*, 1998]. A rough calculation of the stress drop for each event from the maximum slip and approximate radius of its slip areas (Table 2), assuming a circular crack model [*Aki and Richards*, 2002], shows smaller stress drops (3.1–4.9 MPa) for the *M*5.5 13 April 2011 event than the *M*4.7 2008 and *M*5.9 20 March 2011 events (8.5–8.7 and 6.6–7.6 MPa, respectively). Here we used a shear modulus of 50 GPa. Details of the stress drop estimation are explained in the supporting information. The 31 May and 23 September 2011 events also have similarly low stress drops (Table 2). The difference in the waveform characteristics (small differences in acceleration amplitude and large differences in displacement amplitude as shown in Figure 6) may partly be attributed to the difference in the repeaters' stress drops. If we assume the same slip area for the March 2011 (*M*5.9) earthquake as the 2008 (*M*4.7) earthquake instead of our result of the enlarged slip area, the stress drop of the March 2011 earthquake should be 50 times larger than the 2008 event to explain the seismic moment ratio. This leads to an unlikely large stress drop for the March 2011 event given the stress drop for the 2008 earthquake estimated here. Therefore, we conclude that the slip area of the March 2011 earthquake is larger than that of the 2008 earthquake.

The magnitude distribution around the sequence shows that there were no large pre-Tohoku earthquakes near the Kamaishi sequence (Figure 2a). The nearest *M*5 or larger event in the period from 1957 to 2011 was located about 21 km away from the centroids of the Kamaishi sequence. This separation is much larger than the extent of the epicenter distribution of repeaters (3.2 km of standard deviation, which is almost the same as the typical location error for this area) and an enlarged slip area (~8 km) after the Tohoku-oki earthquake. This means that there was no significant seismic slip within the post-Tohoku slip area of the Kamaishi sequence before the Tohoku-oki earthquake. Although the lack of earthquake mean either that itwas locked or slipping aseismicity, if the area surrounding the Kamaishi sequence locked completely, the Kamaishi-oki sequence was unlikely to occur many times before the Tohoku-oki earthquake since the locked area around the Kamaishi sequence shelter the area from tectonic loading. GPS data analyses suggest relatively small locking in this area [e.g., *Suwa et al*., 2006]. Thus, the post-Tohoku slip area expansion suggests that this area, which underwent mostly aseismic slip before the Tohoku-oki earthquake, slipped seismically after it. The seismic slip in the area where pre-Tohoku earthquakes (i.e., the 2008 event) occurred persists both before and after the Tohoku-oki earthquake, but the area to its east varies widely. The eastern slip became smaller and smaller as time passed after the Tohoku-oki earthquake (Figure 10a). This probably indicates that the slip behavior (seismic or aseismic) is strongly dependent on the loading rate in the eastern area because postseismic slip decays rapidly with time.

Matsuzawa et al. [2004] studied the effect of postseismic slip during the earthquake swarm activity in the same subduction zone. In their model, the postseismic slip of an earthquake concentrates stress in other locked areas and promotes (advances) rupture (a chain reaction model). Our results showing an aseismic-to-seismic transition coincident with a fast loading rate indicate that fast loading due to afterslip of a nearby large earthquake not only advances the timing of earthquakes but also increases the seismic moment—an important factor when estimating the hazards of aftershocks caused by large earthquakes. Additionally, if such an aseismic-to-seismic transition occurs during the rupture of a large earthquake, it contributes to expanding the main shock rupture area into the adjacent areas where aseismic slip seems to have been dominant. Although the coseismic rupture processes of large earthquakes may be governed by other physics [e.g., *Noda and Lapusta*, 2013], understanding aseismic-to-seismic transitions is important considering the fact that aseismic slip was observed before the Tohoku-oki earthquake in its coseismic slip area [e.g., *Uchida and Matsuzawa*, 2013].

Next, we discuss how a high stressing rate results in larger earthquake magnitude and slip area. To explain the larger seismic slip area due to a faster loading rate, we consider fault properties governed by a rate- and state-dependent friction law where a, b, and L are parameters that describe the slip behavior [e.g., *Scholz*, 2002]. The slip tends to be unstable if $a - b$ is negative (velocity weakening), while the slip is stable if $a - b$ is positive (velocity strengthening). When $a - b$ is negative, the stability condition depends on critical stiffness K_c [*Scholz*, 2002]:

$$K_c = -\frac{(a-b)\sigma_n}{L} \tag{2}$$

Here σ_n is effective normal stress. Slip is always unstable if stiffness K is smaller than K_c. When K is larger than K_c, that stability depends on the loading rate—slip is stable if the loading rate is small but becomes unstable if the loading rate is large. The state in which the slip behavior depends on the loading rate in a slip rate-weakening region is called conditionally stable [*Scholz*, 2002] or weak seismic [*Boatwright and Cocco*, 1996]. We believe that such a conditionally stable or weak seismic region played an important role in the rupture area expansion of repeaters after the 2011 Tohoku-oki earthquake. In real faults, *Dieterich* [1986] defined a critical fault length l_c:

$$l_c = \eta \frac{GL}{(b-a)\sigma_n} \tag{3}$$

which corresponds to the critical stiffness (K_c) necessary for the occurrence of unstable slip. Here G is shear modulus of the media and η is a nondimensional parameter that depends on the shape of the fault. If the length of a velocity-weakening region ($a - b < 0$) is smaller than l_c, unstable slip cannot occur spontaneously. We drew a conceptual model of the fault properties around the Kamaishi earthquakes in Figure 11. The cumulative slip pattern shown in Figure 10 can be generated when other conditionally stable regions are distributed and separated from the unstable region (the asperity for the 2008 event) by a compliant [*Boatwright and Cocco*, 1996] or weakly stable region ($a - b$ is slightly positive). In such a case and under a small loading rate, seismic slip only occurs in the unstable region (a velocity-weakening region longer than the critical fault length). Such an unstable region is likely responsible for the regular occurrence of the 2008 and other Kamaishi-oki earthquakes before the Tohoku-oki earthquake. The other areas, including the conditionally stable regions, usually show aseismic slip. Under large loading rates such as that caused by the

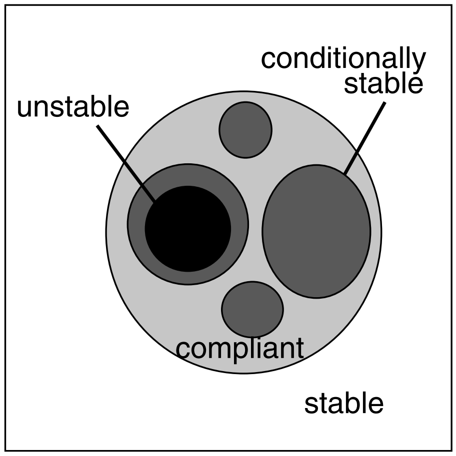

Figure 11. Schematic figure showing fault properties on the plate boundary around the Kamaishi earthquakes. Black, dark gray, light gray, and white areas show unstable, conditionally stable, complaint, and stable areas, respectively.

postseismic slip of the Tohoku-oki earthquake, on the other hand, the whole area except for the stable section ($a - b \gg 0$) can slip seismically.

The critical fault length has also been referred to as the nucleation size, and several equations have been proposed to calculate it [e.g., *Rubin and Ampuero*, 2005; *Scholz*, 2002; *Uenishi and Rice*, 2003]. *Chen et al.* [2010] adopted the following equation for the nucleation size h^* according to *Chen and Lapusta* [2009]:

$$h^* = \left(\pi^2/4\right)GbL/\left[\pi\sigma_n(b-a)^2\right] \tag{4}$$

They demonstrated that a velocity-weakening patch whose radius is comparable to h^* shows clear loading rate dependence of seismic slip in a numerical simulation. They related the loading rate dependence expected from their simulation with the observed changes in seismic moments of repeating earthquakes after the 2004 *M*6.0 Parkfield earthquake. Moment change (increase or decrease) due to increased loading is different depending on the radius and nucleation zone size of the velocity-weakening patch h^*. If a velocity-weakening patch size is comparable to h^*, it shows moment increase with loading rate increase that can explain moment-increased sequences after the Tohoku-oki earthquake. If a velocity-weakening patch size is larger than h^*, it shows weak moment decrease with loading rate increase that can explain moment-decreased sequences. We consider that this model also explains the observed moment change after the Tohoku-oki earthquake.

Although we do not know the fault properties near the Kamaishi and other repeating earthquakes, these studies suggest that a loading rate change can alter the slip behavior of a fault significantly when an earthquake occurs at a velocity-weakening patch with a radius comparable to the nucleation zone size and/or when a conditionally stable region is located near the velocity-weakening area.

5. Conclusions

We found that many repeating earthquake sequences near the downdip edge of the interplate seismic zone showed increases in earthquake magnitude after the 2011 Tohoku-oki earthquake. The magnitude increase averaged 0.3 for sequences with three or more earthquakes each before and after the Tohoku-oki earthquake. The distribution of repeaters with increased magnitude corresponded to the area where large postseismic slip occurred.

In order to study the repeating earthquake size increase mechanism, we examined the seismic activity of the Kamaishi earthquake cluster, where repeating earthquakes with magnitudes ranging from *M*4.7 to *M*5.1 were recognized before the Tohoku-oki earthquake. In that cluster, a significantly larger magnitude event (*M*5.9) occurred 9 days after the Tohoku-oki earthquake. It was followed by four events with *M*5.0 to *M*5.5 within 6 months. From careful phase readings of *P* and *S* waves and double-difference relocation, we obtained a hypocenter distribution of earthquakes that shows alignment probably delineating the plate boundary.

From waveform modeling for the 2008 event and the five events after the 2011 Tohoku-oki earthquake, we found that the slip areas of the five post-Tohoku earthquakes are larger (up to 8 km in diameter) than before (~1.2 km). In the area where slip expanded after the Tohoku-oki earthquake, no significant interplate seismicity had been recognized before. This suggests that the area where aseismic slip was dominant before the Tohoku-oki earthquake slipped seismically after the earthquake. Coupling this with the fact that such magnitude increases were detected for many other repeating earthquakes where the postseismic slip of the Tohoku-oki earthquake was significant, we infer that the increasing loading rate on the patches for repeating earthquake sequences caused the increase in the seismic slip area.

The observed expansion of the seismic slip area under the high loading rate can be explained by the existence of conditionally stable areas near the seismic patches and/or velocity-weakening regions slightly larger than the nucleation length where seismic slip is initiated. Such fault behaviors suggest that aftershock activity around a coseismic slip area is sometimes different from simple triggered seismic slip at previously recognized asperities. The wide distribution of magnitude-increased repeaters suggests that such dependence of seismic slip area size on loading rate is widespread in the case of the Tohoku-oki earthquake. Our results suggest that the areas with conditionally stable property play an important role in determining the size of an earthquake as they change from aseismic to seismic depending on the loading rate.

Acknowledgments
We thank A. Hasegawa and R. Bürgmann for their valuable suggestions and careful reading of the manuscript, T. Kono for his help monitoring the Kamaishi sequence, T. Iinuma and Y. Ohta for the management of GPS data, and R. Nadeau and S. Ide for fruitful discussions. We also thank the NIED for allowing the use of K-NET and KiK-net seismic waveform data, JMA for providing its earthquake catalogue, and GSI for providing GPS data. The constructive review comments from Editor P. Tregoning, Associate Editor, and two anonymous reviewers improved this manuscript very much. This work was supported in part by JSPS KAKENHI 23740328.

References

Aki, K., and P. G. Richards (2002), *Quantitative Seismology: Theory and Methods*, Univ. Science Books, Sausalito, Calif.

Boatwright, J., and M. Cocco (1996), Frictional constraints on crustal faulting, *J. Geophys. Res.*, *101*(B6), 13,895–13,909, doi:10.1029/96JB00405.

Chen, K. H., R. Bürgmann, R. M. Nadeau, T. Chen, and N. Lapusta (2010), Postseismic variations in seismic moment and recurrence interval of repeating earthquakes, *Earth Planet. Sci. Lett.*, *299*, 118–125.

Chen, T., and N. Lapusta (2009), Scaling of small repeating earthquakes explained by interaction of seismic and aseismic slip in a rate and state fault model, *J. Geophys. Res.*, *114*, B01311, doi:10.1029/2008JB005749.

Dieterich, J. H. (1986), A model for the nucleation of earthquake slip, in *Earthquake Source Mechanics*, edited by S. Das, J. Boatwright, and C. H. Scholz, pp. 37–47, AGU, Washington, D. C.

Hartzell, S. H. (1978), Earthquake aftershocks as Green's functions, *Geophys. Res. Lett.*, *5*(1), 1–4, doi:10.1029/GL005i001p00001.

Hartzell, S. H., and T. H. Heaton (1983), Inversion of strong ground motion and teleseismic waveform data for the fault rupture history of the 1979 Imperial Valley, California, earthquake, *Bull. Seismol. Soc. Am.*, *73*(6A), 1553–1583.

Hashimoto, C., A. Noda, T. Sagiya, and M. Matsu'ura (2009), Interplate seismogenic zones along the Kuril-Japan trench inferred from GPS data inversion, *Nat. Geosci.*, *2*, 141–144.

Heki, K., S. Miyazaki, and H. Tsuji (1997), Silent fault slip following an interplate thrust earthquake at the Japan Trench, *Nature*, *386*(6625), 595–598.

Igarashi, T., T. Matsuzawa, and A. Hasegawa (2003), Repeating earthquakes and interplate aseismic slip in the northeastern Japan subduction zone, *J. Geophys. Res.*, *108*(B5), doi:10.1029/2002JB001920.

Iinuma, T., et al. (2012), Coseismic slip distribution of the 2011 off the Pacific Coast of Tohoku Earthquake (*M*9.0) refined by means of seafloor geodetic data, *J. Geophys. Res.*, *117*, doi:10.1029/2012JB009186.

Ishibashi, K. (1999), Great Tokai and Nankai, Japan, earthquakes as revealed by historical seismology: 1. Review of the events until the mid-14th century, *J Geogr.*, *108*(4), 399–423.

Loveless, J. P., and B. J. Meade (2010), Geodetic imaging of plate motions, slip rates, and partitioning of deformation in Japan, *J. Geophys. Res.*, *115*, B02410, doi:10.1029/2008JB006248.

Matsuzawa, T., T. Igarashi, and A. Hasegawa (2002), Characteristic small-earthquake sequence off Sanriku, northeastern Honshu, Japan, *Geophys. Res. Lett.*, *29*, doi:10.1029/2001GL014632.

Matsuzawa, T., N. Uchida, T. Igarashi, T. Okada, and A. Hasegawa (2004), Repeating earthquakes and quasi-static slip on the plate boundary east off northern Honshu, Japan, *Earth Planets Space*, *56*, 803–811.

Murray, J., and J. Langbein (2006), Slip on the San Andreas Fault at Parkfield, California, over two earthquake cycles, and the implications for seismic hazard, *Bull. Seismol. Soc. Am.*, *96*, S283–S303.

Nadeau, R. M., and L. R. Johnson (1998), Seismological studies at Parkfield VI: Moment release rates and estimates of source parameters for small repeating earthquakes, *Bull. Seismol. Soc. Am.*, *88*(3), 790–814.

Nagai, R., M. Kikuchi, and Y. Yamanaka (2001), Comparative study on the source processes of recurrent large earthquakes in Sanriku-oki region: The 1968 Tokachi-oki earthquake and the 1994 Sanriku-oki earthquake, *J. Seismol. Soc. Jpn.*, *54*(2), 267–280.

Nishimura, T., et al. (2000), Distribution of seismic coupling on the subducting plate boundary in northeastern Japan inferred from GPS observations, *Tectonophysics*, *323*, 217–238.

Noda, H., and N. Lapusta (2013), Stable creeping fault segments can become destructive as a result of dynamic weakening, *Nature*, *493*, 518–521.

Okada, T., T. Matsuzawa, and A. Hasegawa (2003), Comparison of source areas of $M4.8+-0.1$ earthquakes off Kamaishi, NE Japan—Are asperities persistent feature?, *Earth Planet. Sci. Lett.*, *213*(3-4), 361–374.

Ozawa, S., T. Nishimura, H. Suito, T. Kobayashi, M. Tobita, and T. Imakiire (2011), Coseismic and postseismic slip of the 2011 magnitude 9 Tohoku-oki earthquake, *Nature*, *475*, 373–376, doi:10.1038/nature10227.

Ozawa, S., T. Nishimura, H. Munekane, H. Suito, T. Kobayashi, M. Tobita, and T. Imakiire (2012), Preceding, coseismic, and postseismic slips of the 2011 Tohoku earthquake, Japan, *J. Geophys. Res.*, *117*, doi:10.1029/2011JB009120.

Rubin, A. M., and J. P. Ampuero (2005), Earthquake nucleation on (aging) rate and state faults, *J. Geophys. Res.*, *110*, B11312, doi:10.1029/2005JB003686.

Rubinstein, J. L., W. L. Ellsworth, K. H. Chen, and N. Uchida (2012), Fixed recurrence and slip models better predict earthquake behavior than the time- and slip-predictable models: 1. Repeating earthquakes, *J. Geophys. Res.*, *117*, B02306, doi:10.1029/2011JB008724.

Scholz, C. H. (2002), *The Mechanics of Earthquakes and Faulting*, Cambridge Univ. Press, Cambridge.

Shimamura, K. (2012), Study on the reproducibity of the interplate earthquakes, PhD thesis, Tohoku Univ., 111 pp.

Shimamura, K., T. Matsuzawa, T. Okada, N. Uchida, T. Kono, and A. Hasegawa (2011), Similarities and differences in the rupture process of the $M \sim 4.8$ repeating-earthquake sequence off Kamaishi, Northeast Japan: Comparison between the 2001 and 2008 events, *Bull. Seismol. Soc. Am.*, *101*, 2355–2368.

Suwa, Y., S. Miura, A. Hasegawa, T. Sato, and K. Tachibana (2006), Interplate coupling beneath NE Japan inferred from three dimensional displacement field, *J. Geophys. Res.*, *111*, B04402, doi:10.1029/102004JB003203.

Tsuji, Y., J. Nakajima, and A. Hasegawa (2008), Tomographic evidence for hydrated oceanic crust of the Pacific slab beneath northeastern Japan: Implications for water transportation in subduction zones, *Geophys. Res. Lett.*, *35*, L14308, doi:10.1029/2008GL034461.

Uchida, N., and T. Matsuzawa (2011), Coupling coefficient, hierarchical structure, and earthquake cycle for the source area of the 2011 off the Pacific coast of Tohoku earthquake inferred from small repeating earthquake data, *Earth Planets Space*, *63*, 675–679.

Uchida, N., and T. Matsuzawa (2013), Pre- and postseismic slow slip surrounding the 2011 Tohoku-oki earthquake rupture, *Earth Planet. Sci. Lett.*, *374*, 81–91.

Uchida, N., A. Hasegawa, T. Matsuzawa, and T. Igarashi (2004), Pre- and post-seismic slip on the plate boundary off Sanriku, NE Japan associated with three interplate earthquakes as estimated from small repeating earthquake data, *Tectonophysics*, *385*, 1–15.

Uchida, N., T. Matsuzawa, A. Hasegawa, and T. Igarashi (2005), Recurrence intervals of characteristic $M4.8 \pm 0.1$ earthquakes off Kamaishi, NE Japan—Comparison with creep rate estimated from small repeating earthquake data, *Earth Planet. Sci. Lett.*, *233*, 155–165.

10.1002/2013JB010933

Uenishi, K., and J. R. Rice (2003), Universal nucleation length for slip-weakening rupture instability under nonuniform fault loading, *J. Geophys. Res.*, *108*(B1), 2042, doi:10.1029/2001JB001681.

Waldhauser, F., and W. L. Ellsworth (2000), A double-difference earthquake location algorithm: Method and application to the Northern Hayward Fault, California, *Bull. Seismol. Soc. Am.*, *90*(6), 1353–1368.

Weldon, R., T. Fumal, and G. Biasi (2004), Wrightwood and earthquake cycle: What a long recurrence record tells us about how faults work, *Geol. Soc. Am.*, *14*, 4–10.

Yamanaka, Y., and M. Kikuchi (2004), Asperity map along the subduction zone in northeastern Japan inferred from regional seismic data, *J. Geophys. Res.*, *109*, B07307, doi:10.1029/2003JB002683.

Ye, L., T. Lay, and H. Kanamori (2012), The Sanriku-Oki low-seismicity region on the northern margin of the great 2011 Tohoku-Oki earthquake rupture, *J. Geophys. Res.*, *117*, B02305, doi:10.1029/2011JB008847.